Scientific Research Publishing

Open Journal of Geology, 2022, 12, 294-311
https://www.scirp.org/journal/ojg
ISSN Online: 2161-7589
ISSN Print: 2161-7570

Mineralogy and Geochemistry of Eteké Eburnean Gold Deposit (Gabon)

Makarim Dalil[1], Nazaire Nzaou Mabika[2], Amina Wafik[2], Zohir Baroudi[1], Abdelmalek Ouadjou[3], Mohamed Gharrabi[3], Amine Bouwafoud[1], Nouamane El Aouad[2], Youssef Zerhouni[1], Saida Alikouss[1]

[1]Laboratoire géosciences et applications, Faculté des sciences Ben M'sik, Casablanca, Morocco
[2]Laboratoire Dynamique de la Lithosphère et Genèse des Ressources, Faculté des Sciences Semlalia, Marrakech, Morocco
[3]Managem Group, Twin Center, Casablanca, Morocco
Email: dalilmakarim@gmail.com

How to cite this paper: Dalil, M., Mabika, N.N., Wafik, A., Baroudi, Z., Ouadjou, A., Gharrabi, M., Bouwafoud, A., El Aouad, N., Zerhouni, Y. and Alikouss, S. (2022) Mineralogy and Geochemistry of Eteké Eburnean Gold Deposit (Gabon). *Open Journal of Geology*, **12**, 294-311.
https://doi.org/10.4236/ojg.2022.123016

Received: December 20, 2021
Accepted: March 28, 2022
Published: March 31, 2022

Abstract

The Gabon geology offered favorable and natural environments for the formation of various types of mineralization. The Etéké gold district, aim of this study, is located in the Ngounié province (southern Gabon) on the western edge of the Chaillu massif. Geologically, the gold mineralization is associated with the Eburnean orogeny and hosted in the Archean greenstone belts. Also, this deposit is covered by a significant vegetation cover and a very extensive lateritic weathering profile, which hinders the most accurate study. Through this paper, we aim to propose a genesis pattern of this mineralization via a multidisciplinary approach. To do this, a petrographic, metallogenic, and geochemical characterization has been established in the different sectors of the Etéké deposit. The studied deposits display varied facies which are encased in granitoid. They are essentially formed of abundant granitoid, and amphibolite compared to the volcano-sedimentary formations. These rocks display magmatic textures, affected by metamorphism, and not sufficiently preserved. Based on our multidisciplinary approach, the studied samples collected from the core's boreholes allowed us to decipher a volcanogenic and metamorphosed origin of the gold genesis.

Keywords

Eburnean Orogeny, Gabon, Gold, Greenstone, Granitoids, Amphibolite

1. Introduction

1.1. Geology of Gabon

The examination of the Gabon map helps to differentiate four major tectono-

stratigraphic sets [1] designated in a regional context. From the bottom to the top, we found the Archean basement, the Paleoproterozoic formations, the Neoproterozoic of Nyanga, and the Phanerozoic groups (**Figure 1**):

- The Archean domain, part of the Congo craton, extends from Congo to Cameroon crossing Gabon and represent the Precambrian basement of the central Africa [2] [3]. It consists of Archean cratons welded together by the Mesoproterozoic and Paleoproterozoic belts [4] [5] and represented mainly, in the Gabon territory, by the Chaillu massif and the North Gabon massif. Its establishment is the result of significant magmatic activities that led to the formation of diverse ultrabasic and granitoid rocks that are the subject of several datations in the Chaillu massif [1] [6] [7] [8].

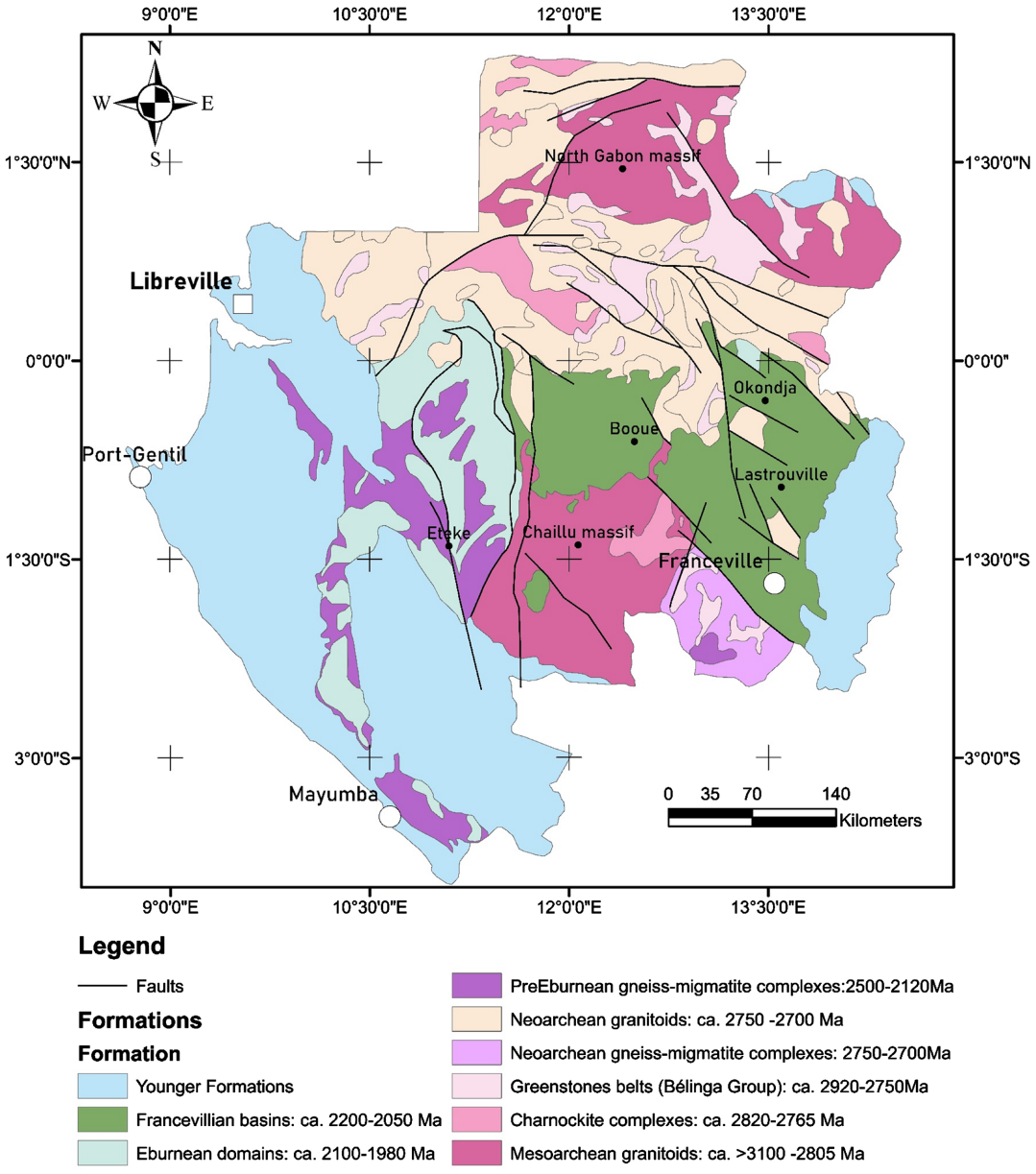

Figure 1. Simplified geological map of Gabon, defining the main structural domains (modified [1]).

- The Paleoproterozoic domain is the result of the collision between the Congo and Sao Francisco cartons during the Eburnean orogeny (2500 - 2000 Ma) [9] [10] [11]. In Cameroon, Central Africa, Congo and more particularly Gabon, the Eburnean orogeny has been recognized by a folded belt similar to the Phanerozoic belt dominated by modern plate tectonics [1] [12] [13]. In the central part of Gabon, this belt is characterized by the Ogooué mobile zone and particularly by the establishment of intracratonic basins in the Francevillian such as the Booué, Lastourville, Okouja and Franceville basins (**Figure 1**) [10] [12] [14] [15] [16] [17]. These basins lay in discordance on the Archean base of the Chaillu massif. The well-known basin is the Franceville basin, since it contains manganese deposits [18] [19] [20] [21] and uranium [15] [16] [22].
- The Neoproterozoic domain includes geological formations represented by the Mayombe-African belt which dominates in the south of the country. This belt is formed by massive Paleoprotezoic granite covering the Neoprotezoic deposits of the Pan-African foreland basin [23].
- The Phanerozoic domain outcrops in the West at the location of the coastal basin linked to the opening event of the South Atlantic Ocean during the Lower Cretaceous [24] and in the East at the location of the Paleogene to Quaternary sandstones and the aeolian sands of the Batéké plateau [8] [25].

1.2. Geological Situation, Location and Description of the Eteké Gold Showings

From 1937 to 1959, the Eteké gold district, located in southern Gabon, was the primary source of gold production in the country. Several tons of alluvial gold were extracted [11] mostly in the Dando-Mobi sectors (ore of 2.3 - 7.2 t grading 15 g/t), Ovala (ore 2 t grading 11 g/t) and Dango (5.8 t grading 8.4 g/t and ore 8.4 grading 2.4 - 9.8 g/t). This corresponds to gold veins set up at the time of the Paleoproterozoic Eburnean orogeny between 2.0 and 2.2 Ga [26] and hosted in the greenstone belts of Archean ages of the Chaillu massif (Congo Craton) [1] [27]. These green rocks are essentially formed from amphibolites traversed by granitoid intrusions [1] [28].

In the Eteké region, the gold mineralization is linked to the Eburnean orogeny and it is the most interesting in this deposit category. Five primary sites have been recognized in the Etéké region (**Figure 2**) and will be the subject of our study:

- Dondo-Mobi: Prospect essentially hosted in ultrabasic rocks of the Etéké group, located between the thrust plane and the Staurolite mica schists of the Ogooué supergroup [28].
- Dango: The supporting bedrock of the Dango deposit is mainly composed of sedimentary rocks from the Massima supergroup [28]. The lithological terms are represented by black muscovite-chlorite schists and jasper recrystallized into massive or banded quartzites.
- Ovala: District located in a Paleoproterozoic syncline, wedged between two

Figure 2. ((a) and (b)) Example of SIM affecting the tectonic fabric; (c) Opening and displacement of the expansion zone filled with iron carbonates; ((d) and (e)) Quartz veins intersecting the SIM silicified foliation; ((f) and (g)) Mineralized zones characterized by SIM with cubic pyrites; (h) Brechiated zone superimposed on the SIM with cement hematite.

domes of remobilized Archean migmatites [28]. This synclinal filling is filled with sediments and lavas from the Etéké group, the Massima and Ogooué supergroups.

2. Material and Methods

The Etéké gold district is characterized by significant vegetation cover and a well-extended lateritic alteration profile. Core drillings data were therefore of paramount input to our study, as they enabled us to define the relationships be-

tween host rocks and mineralized veins.

Therefore, a total of 700 rock samples from 106 core holes from the study area were used to make the thin sections, the polished section and to perform the geochemical analyzes. Petrographic and metallogenic examinations were carried out by the optical microscope and the metallographic microscope within the Faculty of Sciences Semlalia University Cadi Ayyad Marrakech, and Faculty of Sciences Ben M'sik University Hassan II Casablanca, in order to define the mineral phases as well as the metallic phases and determine their relationship with the surrounding area. Also, analyses on total rocks in major and trace elements by ICP-AES and ICP-MS were respectively carried out at the REMINEX research center and laboratory in Marrakech, respectively, using a Horiba Jobin Yvon ULTIMA 2c and Thermo-fisher X series 2 spectrometers.

3. Results and Discussion

3.1. Description of Eteké Gold Prospects

3.1.1. Dango Zone

The Dango zone corresponds to a zone with significant, massive and whitish silicification (**Figure 2(a)**, **Figure 2(b)**) (SIM: silicification, intense and massive). The development of this SIM is synchronous with the deformation, on the basis that the tectonic fabric is permeated in the silicification.

The silica impregnation is recognized, which generates textures in flames or lenses. The red-orange hues are largely related to iron carbonates and fill the compatible working thickness with a shear play indicative of tectonic movement during the silicification and iron carbonate impregnation (**Figure 2(c)**). The quartz veins which intersect the silicification suggest a genetic link with the main mineralization zone (**Figure 2(d)**, **Figure 2(e)**). The mineralization takes the form of total silicification, whitish with cubic pyrites (**Figure 2(f)**, **Figure 2(g)**). It overlaps with an episode of SIM breccia expressed by fine cement hematitization (**Figure 2(h)**).

3.1.2. Dondo-Mobi Zone

The Dondo-Mobi deposit has been known for its mineralization associated with hydrothermal alteration by the biotite and quartz veins. The metamorphosed volcano-sedimentary host is relatively homogeneous with a microgranular texture with andesitic compositions (**Figure 3(a)**, **Figure 3(c)**). Here, the deformation is well defined and expressed by an alignment of metamorphic biotite. Locally, the silicification of the host is accentuated in the vicinity of the tourmaline-pyrite zones (**Figure 3(b)**) ant the hydrothermal alteration is manifested by the random distribution of biotites in the foliation, indicating low foreshortening deformation under high fluid pressure (**Figure 3(d)**).

3.1.3. Ovala Zone

The Ovala deposit has been characterized for its dominant clastic sedimentary rocks, highly developed muscovite schists, extensive silicification, and kyanite

porphyroblasts. Here, Muscovite schist is the most dominant feature, but represents an epiphenomenon to mineralization. The muscovite is nested within each other, revealing no deformation (Figure 4(a)) and clearly intersecting pyrites (Figure 4(b)). The presence of kyanite porphyroblast indicates a superimposed metamorphism on bleached rocks. This is a typical feature of metamorphosed volcanogenic deposits into amphibolite facies (Figure 4(c)).

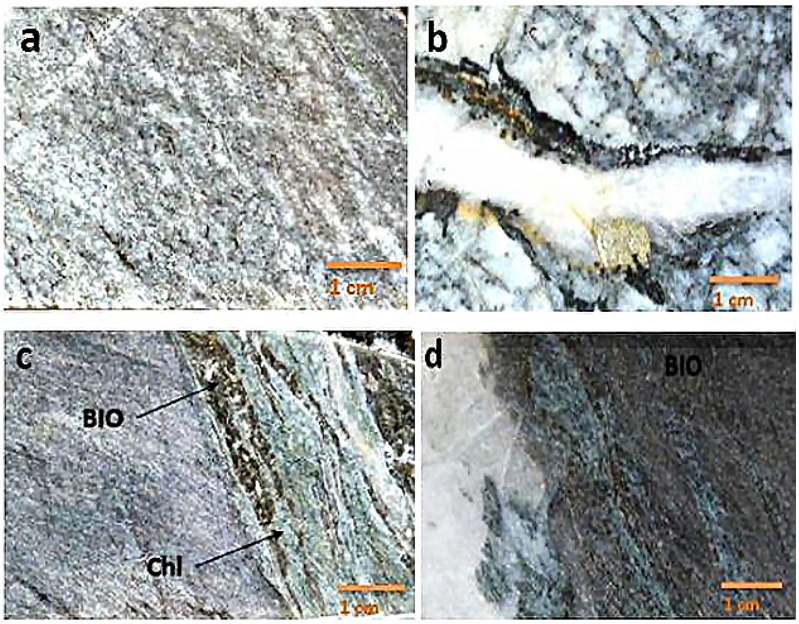

Figure 3. (a) Massive appearance of andesites; (b) Silicified zone within andesites, with quartz passages, tourmaline and pyrite development/Different manifestations of biotite (c) in impregnation of volcano-sedimentary; (d) in impregnation in schistosity planes.

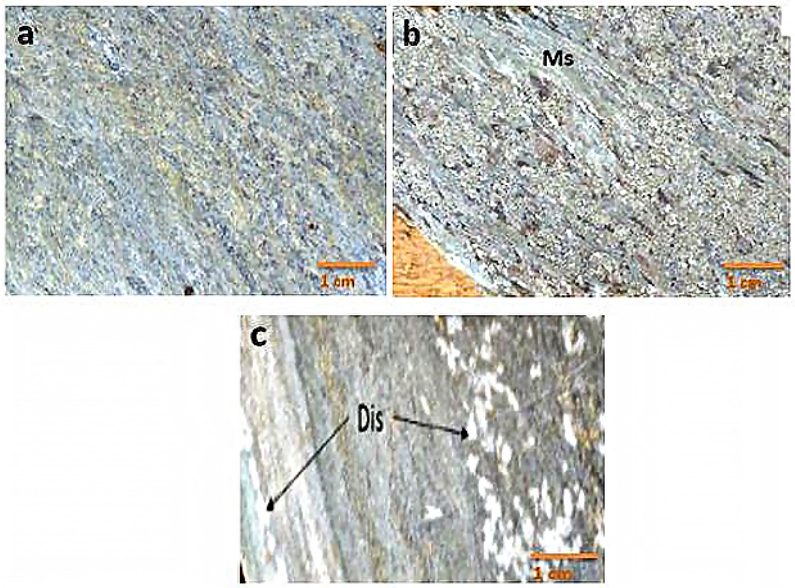

Figure 4. (a) Interconnected muscovites without evidence of deformation; (b) Muscovite schist clearly intersecting pyrites; (c) Kyanite porphyroblasts; (d) is developed on finely bedded detrital sedimentary rocks.

3.1.4. Massima Zone

The studied cores in the Massima district expose a volcano-sedimentary sequence (Figure 5(a)) injected into mafic sills. These rocks are weakly deformed, except in the graphitic shales zones they present a very strong deformation (Figure 5(b)). These boreholes contain several gold zones closely related to disseminated pyrite in the silicified volcano-sedimentary zones (Figure 5(c)).

3.1.5. Moukanda Zone

In this study area, the treated boreholes display gabbroic sequences with particle size varying from microgranular to granular. The invasion of the structural fabric seems to have a link with the grain size: the less grainy parts are the least affected by the deformation. Probably, it could be due to the metamorphic recrystallization.

3.2. Petrographic and Metallographic Characterizations of the Study Area

The Etéké Gold deposit represents a wide facies variety, it is encased in granitoids. These rocks have been located in the base of the Chaillu massif, and characterized with a magmatic texture that are not sufficiently preserved and affected by metamorphism. The samples prepared from the core's boreholes allowed us to determine the different facies below:

3.2.1. Sandy Chloritized Metapelite

It is a very thin facies composed of micaceous and sandy levels. These levels are composed of very fine crystals of quartz, intensely recrystallized and flattened according to the regional schistosity (Figure 6(a)). Some white micas also appear

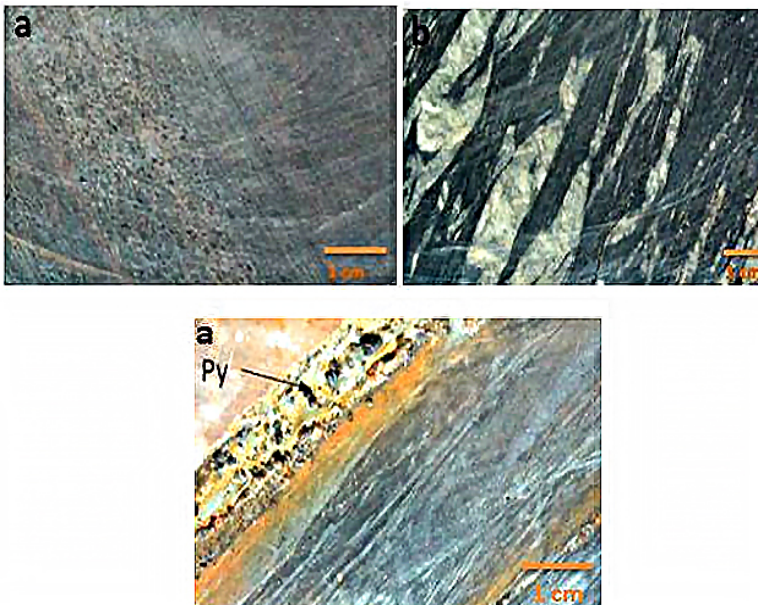

Figure 5. (a) Volcano-sedimentary sequence; (b) well-deformed graphitic shales with folding and boudinage of siliceous ribbons; (c) Ribbons of pyrite (Py) developed along the bedding.

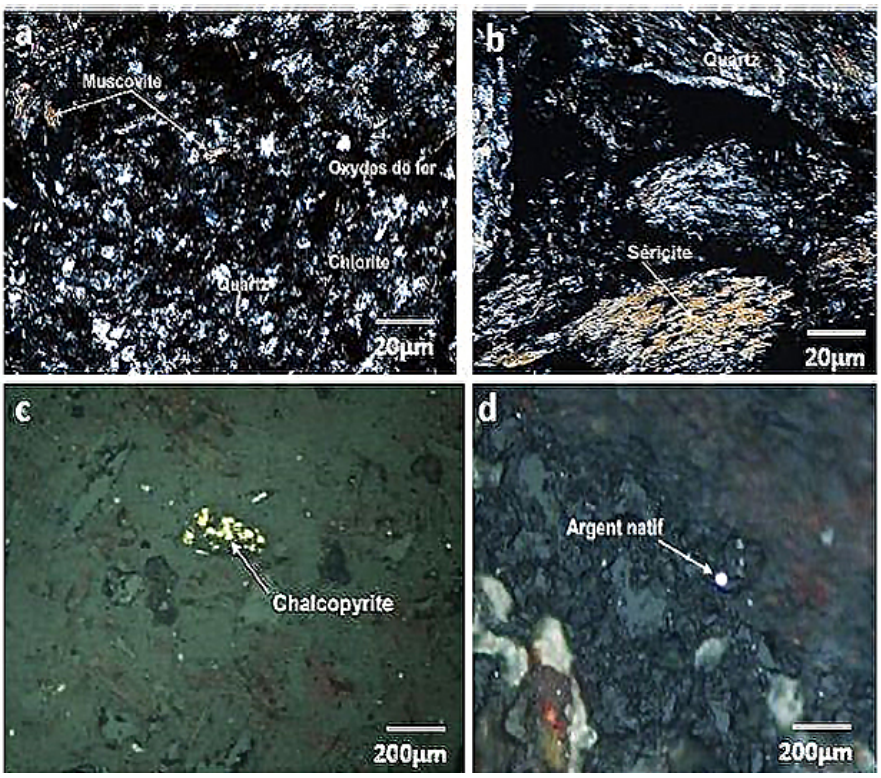

Figure 6. (a) Microscopic bservation of sandstone levels (LP); (b) Micaceous fragment in the pelitic level (LN); (c) Dissemination of chalcopyrite in the sandstone level (LN); (d) Silver grain (LN).

in these levels.

The micaceous levels are dominated by sericite and muscovite. These micas are generally oriented according to the regional schistosity (**Figure 6(b)**). In the vicinity, the white micas are strongly folded and attest the presence of a late deformation phase. Also, there is a strong chloritization of the rock which is manifested by a development of chlorite instead of the white micas. Opaque minerals are very abundant in this facies, giving it a reddish appearance.

From a metallogenic point, this facies contains chalcopyrite in ranges (50 to 100 µm), disseminated (**Figure 6(c)**), some very fine grains of arsenopyrite (<50 µm) and very fine droplets (<5 µm) of silver (**Figure 6(d)**). We also note the presence of grains and granules of iron oxides (20 - 200 µm) strongly disseminated in the rock.

3.2.2. Rubefied Quartzite

This facies have gathered mainly intense recrystallized quartz. The mineralogy observed indicates that the fragments of the studied rock would correspond to a quartzite. Nevertheless, some fragments with the same mineralogy but their particle size is coarser would correspond to quartz veins or faults that have been deformed in the same way as quartzite (**Figure 7(a)**). The rock cement is siliceous, more or less reddened (**Figure 7(b)**, **Figure 7(c)**).

Indeed, it is strongly impregnated with iron oxides which has been invaded in

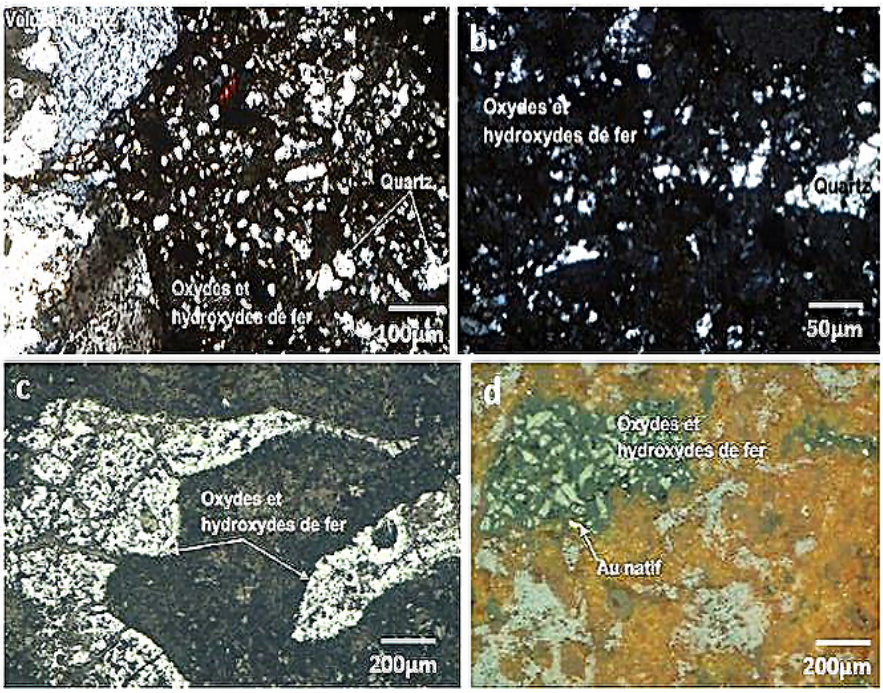

Figure 7. (a) reddened quartzite and quartz veins (LN); (b) Microscopic appearance of quartz crystals with oxides cement (LN); (c) Mass of oxids observed in the facies (LN); (d) Golden grain (Au natif) in association with iron oxides (LN).

the fragments by the fractures and cracks that affect them. This facies are characterized by a strong impregnation of iron oxides in the form of micrometric to millimeter ranges covering the entire rock (**Figure 7(d)**).

3.2.3. Meta-Andesite

This rock shows a microlithic porphyry texture (**Figure 8(a)**, **Figure 8(b)**) whose mineralogy is formed by:

- Quartz in the form of crystals, recrystallized and forms the cryptocrystalline matrix of the rock.
- The Feldspar, which is more or less abundant in these facies, is corroded at the edge. Its peripheries are frequently confused with the quartzo-feldspar matrix. Its size varies from 200 to 500 µm. It is usually very altered with a characteristic dirty appearance (**Figure 8(c)**).
- The weathering minerals observed are quartz, chlorite and white micas.
- The Plagioclase is relatively abundant in these facies. It is in the form of crystals of variable size (a few microns to 1 mm). They often have polysynthetic twin, and sometimes are strongly altered in chlorite, calcite, and epidote.
- The amphibole, dark green to light in color, is either in the form of ranges, micrometric to millimeter dimension, with cross-sections and longitudinals of greater dimension, or in the form of clusters with several combined ranges (**Figure 8(a)**, **Figure 8(c)**).

The cryptocrystalline matrix of the rock is represented by very chloritized quartz-feldspar nature. This chloritization, giving the rock a characteristic

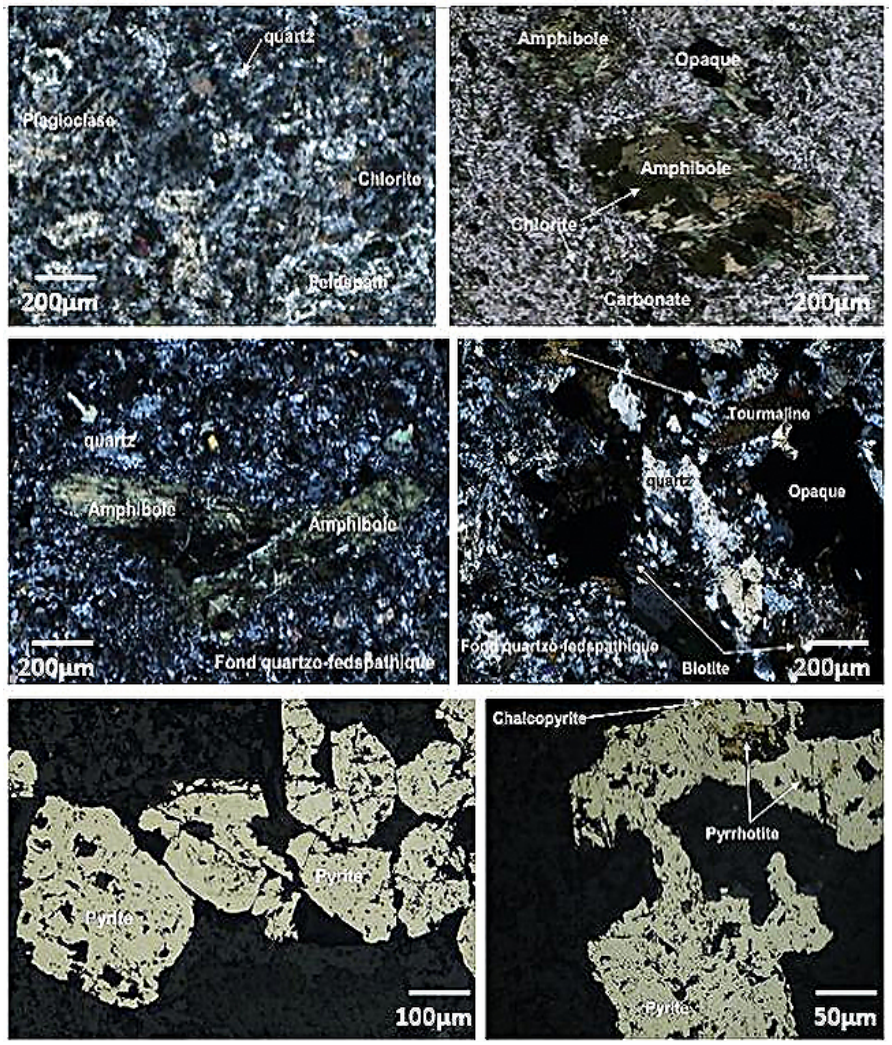

Figure 8. (a) Meta-andesite (LP); (b) Amphibole observed in meta-andesite (LN); (c) Amphibole sections observed in meta-andesite (LP); (d) Microscopic appearance of sulfo -quartz vein (LP); (e) Microscopic view of pyrite in meta-andesite (LN); (f) Fine inclusions of chalcopyrite within pyrites (LN).

greenish appearance, is interpreted by a massive development of chlorite, in isolated or massive flakes developing on biotites, amphibole and on the matrix. In addition, we still note the presence of the epidote in finely disseminated granules, sometimes grouped. Carbonates completely invade the matrix, attesting to a late carbonation (**Figure 8(d)**).

From a Metallography view, the pyrite is very abundant in this facies, in the form of isolated crystals (50 to 500 µm) automorphic to xenomorphs finely disseminated in the rock; or grouped into several individuals, sometimes forming masses exceeding 1 mm (**Figure 8(e)**). These pyrite masses, in combination with quartz and carbonates, fill the fractures affecting the rock. Chalcopyrite has also been observed in this facies. It is in the form of ranges of dimensions from 50 to 200 µm, associated with pyrite and quartz at fractures, affecting the rock. Locally, it appears either in the form of scattered beaches; or in very fine inclusions

within pyrite (Figure 8(f)).

3.2.4. Amphibolite

It is a deformed, recrystallized facies slightly oriented according to the direction of foliation. It is recognized by the following mineralogy: amphibole, biotite, chlorite, calcite and quartz. The Amphiboles are very common (Figure 9(a)), they are in the form of elongated crystals according to the direction of foliation. Some crystals have a Poikilitic texture. Chlorites exhibit a radio-fibrous form (Figure 9(b)) and biotites present in a fibrous aspect are also visible in the rock (Figure 9(b)).

In these facies, the Quartz, slightly present, are recrystallized forming triple points with rolling extinction and corroded by the matrix of the rock. However, Calcite is abundant and permeates the entire rock (Figure 9(c)). Under a metallographic microscope, this structure shows the presence of very fine iron hydroxide boundaries in the late cracks and fractures and very fine grains (<5 μm) of Gold and/or Silver have been also observed in quartz (Figure 9(d)).

3.3. Whole Rock Geochemistry: Classification and Geodynamic Settings

3.3.1. Volcanics Rocks

The composition of the analyzed samples follows that of mafic rocks characterized by relatively low SiO_2 contents (43.35 wt% to 55.5 wt%). MgO content varies

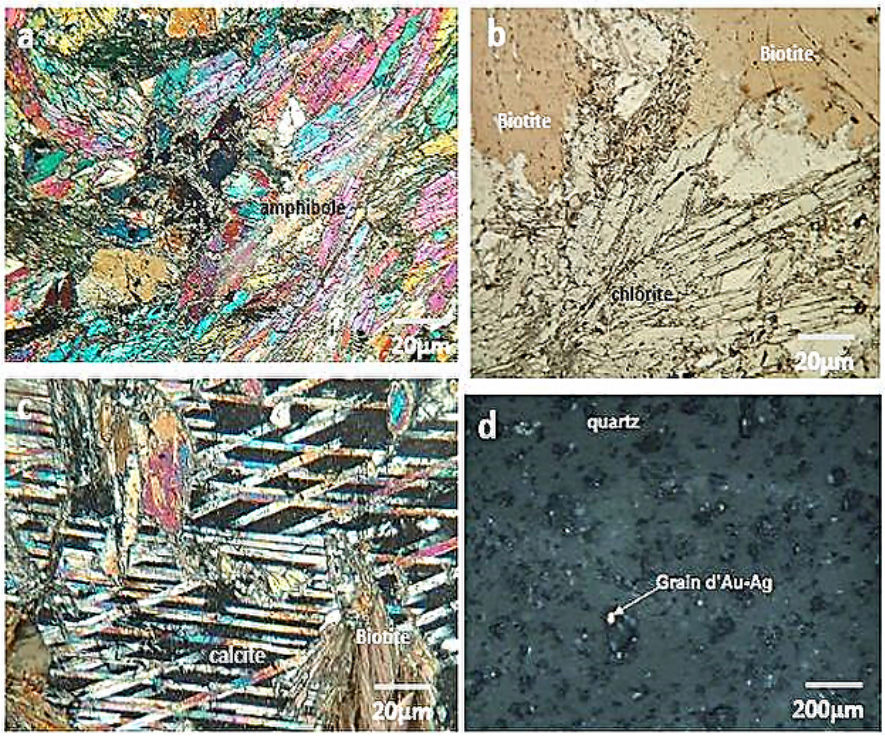

Figure 9. (a) Amphibole sections stretched along the deformation direction; (b) Chlorite and biotite range in the amphibolite (LN); (c) Impregnation of calcite on rock (LP); (d) Ag-Au grain in quartz.

from 3.82 wt% to 22.42 wt% and the Al_2O_3 content varies from 6.39 to 18.85 wt.%. The results also highlighted a high content of FeOt (7.17 wt% - 12.54 wt%) and CaO (3.64 wt% - 13.41 wt%), while the contents of MnO (0.13 wt% - 0.18 wt%), P_2O_5 (0.04 wt% - 0.11 wt%) and TiO_2 (0.41 wt% - 0.76 wt%) are considerably lower. The studied rocks show high contents of Sr (35 - 310.8 ppm), Zr (15.9 - 84.9 ppm), Ni (16.9 - 688.6 ppm), and Cr (29.9 - 1550 ppm). Based on the diagram of [29], the rock samples have predominantly basaltic and basaltic-andesite rock compositions (**Figure 10**).

On the Zr-MgO diagram, all the samples are discriminated to be ortho-amphibolite (**Figure 11(a)**). The studied rocks have a calc-alkaline affinity (**Figure 11(b)**) and they exhibited arc-basalt setting (**Figure 11(c)**). Trace element contents of the studied samples were also used to determine the possible tectonic setting of the rocks. The distribution of our samples on the triangular diagram of [30], shows that our amphibolites are predominantly grouped in the volcanic-arc basalts setting of the orogenic domain (**Figure 11(d)**).

3.3.2. Granitoïds

The studied granitoid samples consist of SiO_2 (57.66 wt% - 69.51 wt%), 0.59 wt% - 4.08 wt% of K_2O, and significant concentrations of Al_2O_3 (15.77-19.18 wt.%), Na_2O (0.39 wt% - 5.29 wt%), FeOt (2.76 wt% - 7.8 wt%) and MgO (0.81 wt% - 2.82 wt%). As for the trace metal content, these rocks showed high levels of Sr (14 to 341.1 ppm), Rb (28.3 to 341.9 ppm) and Y (up to 26.6 ppm), leading to a low to moderate Sr/Y ratio (2.09 to 51.68 ppm). According to the geochemical classification diagram of (Middlemost, 1994), our granitoid classifies as diorite

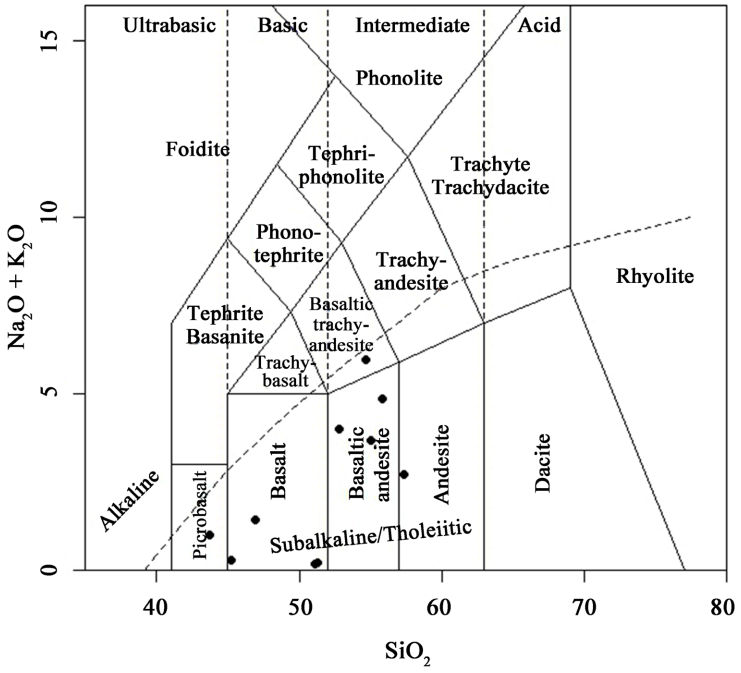

Figure 10. Total alkaline-silica (TAS: [29]) diagram for the volcanic rocks of the Etéké gold district.

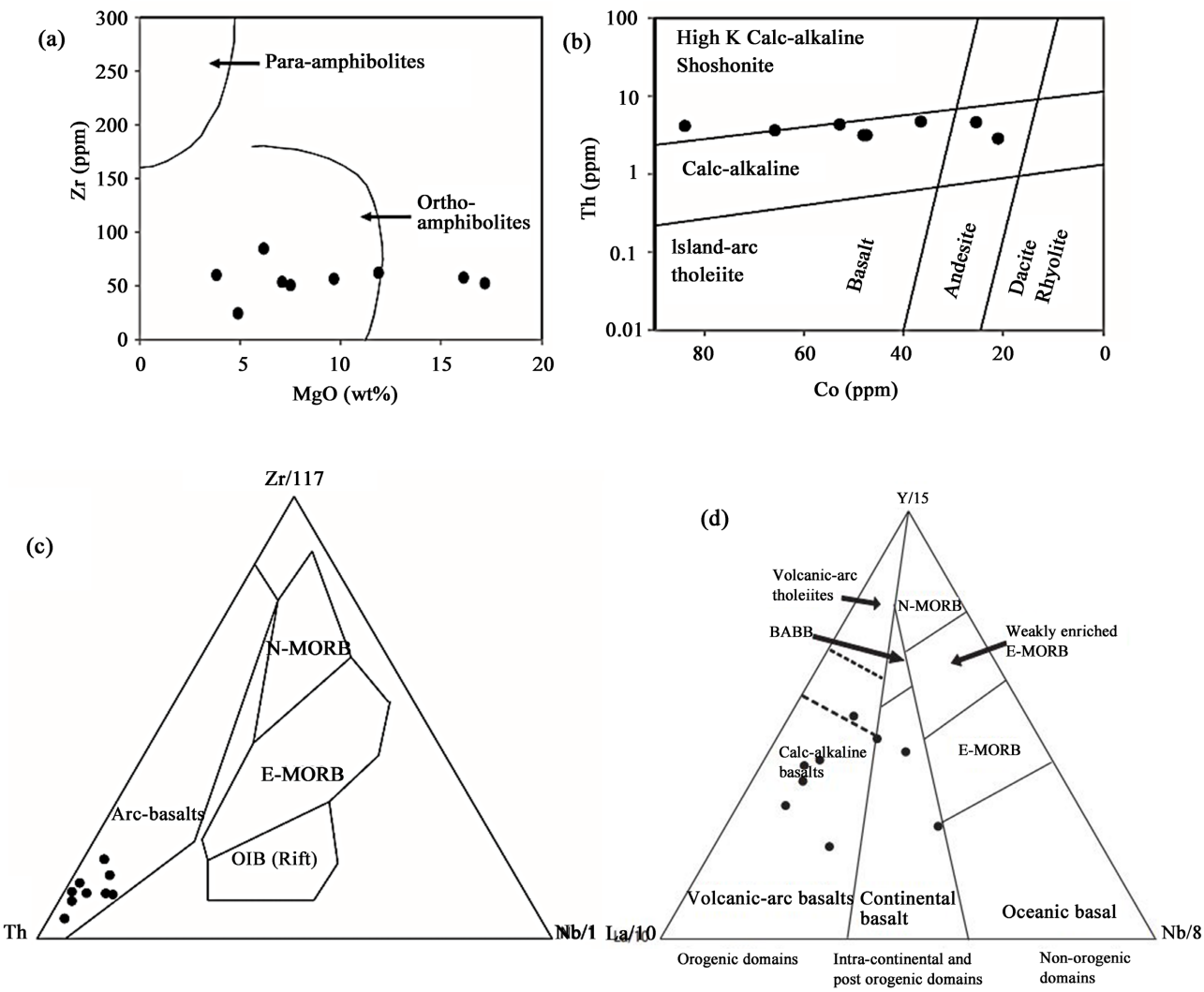

Figure 11. (a) Zr vs. MgO [31]; (b) Th vs. Co [32]; (c) Th–Hf/3–Ta [33] and (d) La-Y-Nb [30] diagrams for the amphibolite samples.

and granodiorite when using the classification of Middlemost (**Figure 12**).

The granitoids samples, characterized by a diorite to granodiorite geochemical composition, are predominantly calc-alkaline and moderately to highly potassic rocks (**Figure 13(a)**). The nature of these rocks is also found to be metalliferous to peraluminous (**Figure 13(b)**). Furthermore, the projection of these rocks in the diagram of (Pearce *et al.*, 1984) indicates that all the studied granitoid samples are classified in the volcanic arc granitoid (VAG) domain (**Figure 13(c)**, **Figure 13(d)**). These geochemical characteristics indicate that the Etéké granitoids could be derived from the partial melting of hydrated basaltic crust in subduction zones and from garnet and/or amphibole residues [34] [35] [36] [37].

4. Conclusions

The geological history of Gabon provides information on the formation of several strategic natural resources with valuable economic interest (gold, manganese, iron, etc.). Gabonese gold, aim of this study, is produced intermittently and

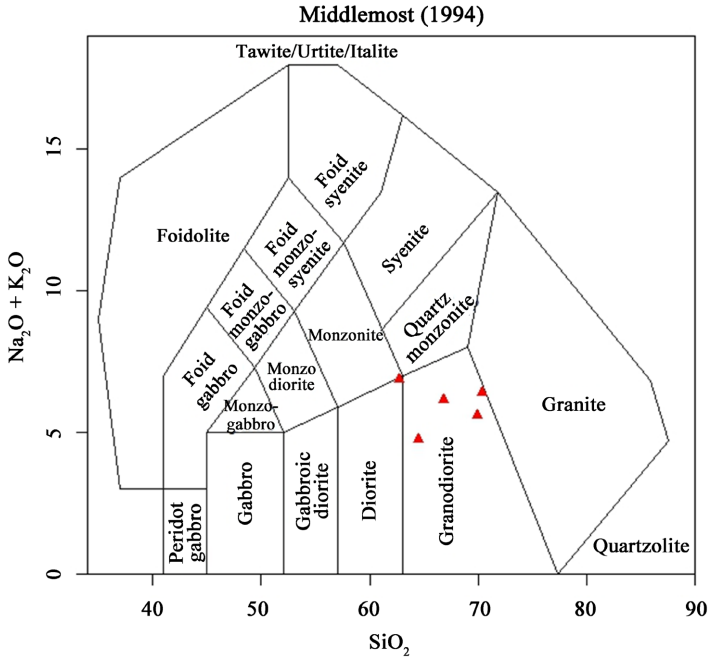

Figure 12. Classification diagram [38] of the granitoïds from Etéké gold district.

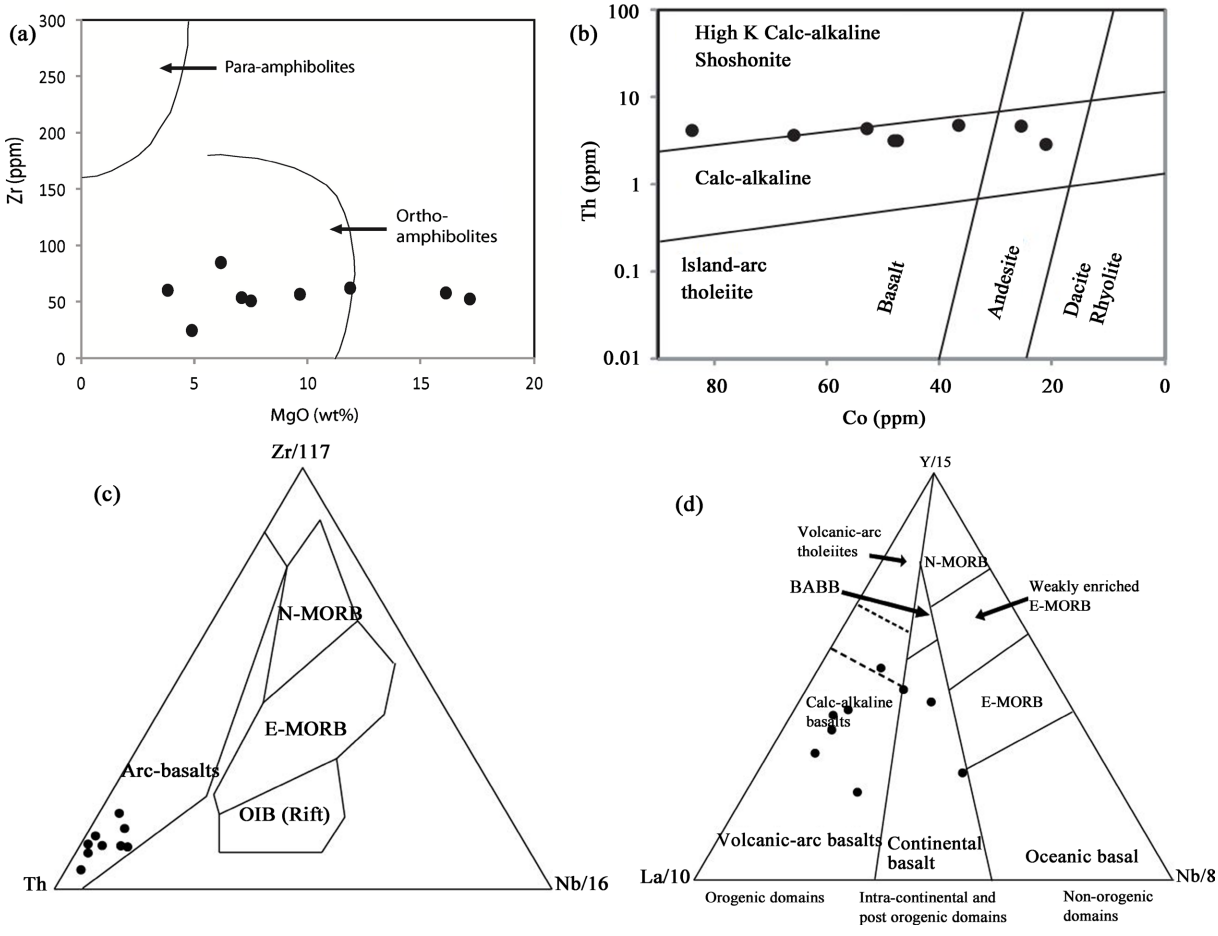

Figure 13. K_2O vs. SiO_2 diagram [39]; (b) A/CNK–A/NK diagram [40] and ((c), (d)) Tectonic discrimination diagrams [41] for the Etéké granitoïd samples.

generated mainly from the Etéké region.

In the Eteké region, the gold mineralization is linked to the Eburnean orogeny. The Etéké gold districts display considerably significant alteration. The most common alterations are carboniferous and silicified impregnations. Otherwise, the ferriferous oxidations prove to be the major characteristic in certain deposits. Five primary sites have been characterized in the Etéké region:

- Dango zone: it is well-known by a SIM whose origin is synchronous with the deformation, on the basis of the tectonic fabric which is permeated in the silicification. this deposit corresponds to an orogenic mineralization system with significant silicification during shearing.
- Dondo-Mobi zone: it represents a characteristic orogenic system formed by weak tectonic shortening and a usual geometry of sub-horizontal stress veins and more inclined shear veins. Random biotite is the hydrothermal alteration mineral as the mineralization was emplaced at slightly elevated temperatures.
- Ovala zone: It exhibits the opposite characteristics genetically. For example, the predominant element, muscovite shale, is not associated with gold mineralization. On the other hand, the high silicification, the pyritization in sterile zones and gold-bearing zones, parallel to the bedding and essentially the occurrence of kyanite porphyroblasts fit perfectly into a model of metavolcanogenic gold mineralization.
- Massima deposit: it is typically part of volcanogenic systems, this results in the disseminations of pyrites in volcano-sediments separated by late sills and also the unit of mineralized basalt with silicified gold zones with black chlorite.
- Moukanda prospect: it is characterized by the biotite abundance (source of the fabric), the upper green schist facies which is belonged to the metamorphism and some parts downgraded to chlorite

Petrographic and geochemical characterization of amphibolite and granitoid samples from the Etéké gold district were used to define their petrogenesis and tectonic frameworks. Therefore, we can retain:

- The studied volcanic rocks show geochemical compositions of basalt to basaltic andesite;
- The geochemical signature indicates that the Eteké amphibolite are basaltic arc and probably originate from a subduction zone;
- The studied granitoids show a geochemical evolution from diorite to granodiorite and would come from the partial melting of the hydrated basaltic crust in the subduction zones.

Conflicts of Interest

The authors declare no conflicts of interest regarding the publication of this paper.

References

[1] Thiéblemont, D., Castaing, C., Billa, M., Bouton, P. and Preat, A. (2009) Notice

explicative de la carte géologique et des ressources minérales de la République Gabonaise à 1/1000000. *Programme Sysmin*, **8**, 384.

[2] Toteu, S.F., Michard, A., Bertrand, J.M. and Rocci, G. (1987) U/pb Dating of Precambrian Rocks from Northern Cameroon, Orogenic Evolution and Chronology of the Pan-African Belt of Central Africa. *Precambrian Research*, **37**, 71-87. https://doi.org/10.1016/0301-9268(87)90040-4

[3] Nedelec, A., Nsifa, E.N. and Martin, H. (1990) Major and Trace Element Geochemistry of the Archaean Ntem Plutonic Complex (South Cameroon): Petrogenesis and Crustal Evolution. *Precambrian Research*, **47**, 35-50. https://doi.org/10.1016/0301-9268(90)90029-P

[4] De Waele, B., Johnson, S.P. and Pisarevsky, S.A. (2008) Palaeoproterozoic to Neoproterozoic Growth and Evolution of the Eastern Congo Craton: Its Role in the Rodinia Puzzle. *Precambrian Research*, **160**, 127-141. https://doi.org/10.1016/j.precamres.2007.04.020

[5] De Wit, M.J. and Linol, B. (2015) Precambrian Basement of the Congo Basin and Its Flanking Terrains. In: De Wit, M. and Guillocheau, F., Eds., *Geology and Resource Potential of the Congo Basin*, Springer, Berlin, 19-37. https://doi.org/10.1007/978-3-642-29482-2_2

[6] Caen-Vachette, M., Vialette, Y. Bassot, J.P. and Vidal, P. (1988) Apport de la géochronologie isotopique à la connaissance de la géologie gabonaise. *Chronique de la Recherche Minière*, No. 491, 35-54.

[7] Chevallier, L., Makanga, J.F. and Thomas, R.J. (2002) Notice explicative de la Carte géologique de la République Gabonaise a 1/1 000 000. Editions DGMG, Libreville.

[8] Bouton, P., *et al.* (2009) Notice explicative de la carte géologique de la République du Gabon a 1/200 000, feuille Franceville-Boumango. Editions DGMG, Libreville.

[9] Mayaga-Mikolo, F. (1996) Chronologie des evenements sedimentaires, magmatiques et tectono-metamorphiques du precambrien d'afrique centrale occidentale (Gabon): Tectogenese ogooue et heritage archeen. BRGM, Orléans.

[10] Feybesse, J.L., *et al.* (1998) The West Central African Belt: A Model of 2.5-2.0 Ga Accretion and Two-Phase Orogenic Evolution. *Precambrian Research*, **87**, 161-216. https://doi.org/10.1016/S0301-9268(97)00053-3

[11] Bouchot, V. and Feybesse, J.L. (1996) Palaeoproterozoic Gold Mineralization of the Etéké Archaean Greenstone Belt (Gabon): Its Relation to the Eburnean Orogeny. *Precambrian Research*, **77**, 143-159. https://doi.org/10.1016/0301-9268(95)00047-X

[12] Ledru, P., Johan, V., Milési, J.P. and Tegyey, M. (1994) Markers of the Last Stages of the Palaeoproterozoic Collision: Evidence for a 2 Ga Continent Involving Circum-South Atlantic Provinces. *Precambrian Research*, **69**, 169-191. https://doi.org/10.1016/0301-9268(94)90085-X

[13] Lerouge, C., *et al.* (2006) Shrimp U-Pb Zircon Age Evidence for Paleoproterozoic Sedimentation and 2.05 Ga Syntectonic Plutonism in the Nyong Group, South-Western Cameroon: Consequences for the Eburnean-Transamazonian Belt of NE Brazil and Central Africa. *Journal of African Earth Sciences*, **44**, 413-427. https://doi.org/10.1016/j.jafrearsci.2005.11.010

[14] Weber, F. (1968) Une série précambrienne du Gabon: Le Francevillien. Sédimentologie, géochimie, relations avec les gites minéraux associés. *Sciences Géologiques, Bulletins et Mémoires*, **28**, 328 p.

[15] Bourrel, J. and Pfifelmann, J.P. (1974) The Uraniferous Province of the Franceville Basin (Gabon Republic) Africa. Broken Hill Proprietary Co., Ltd., Shortland, 1-18.

[16] Gauthier-Lafaye, F. (1986) Les gisements d'uranium du Gabon et les réacteurs d'Oklo. Modèle métallogénique de gîtes à fortes teneurs du Protérozoïque inférieur. *Sciences Géologiques*, *Bulletins et Mémoires*, **78**, 226 p.

[17] Zhao, G., Cawood, P.A., Wilde, S.A. and Sun, M. (2002) Review of Global 2.1-1.8 Ga Orogens: Implications for a Pre-Rodinia Supercontinent. *Earth-Science Reviews*, **59**, 125-162. https://doi.org/10.1016/S0012-8252(02)00073-9

[18] Baud, L. (1954) Carte géologique de reconnaissance à 1/500 000. Feuille de Franceville-Est avec notice explicative. *Bulletin de la Direction des mines et de la géologie de l'AEF*, **221**, 260-261.

[19] Bouladon, J., Weber, F., Veysset, C. and Favre-Mercuret, R. (1965) Sur la situation géologique et le type métallogénique du gisement de manganèse de Moanda, près de Franceville (République Gabonaise). *Sciences Géologiques*, *Bulletins et Mémoires*, **18**, 253-275. https://doi.org/10.3406/sgeol.1965.1293

[20] Leclerc, J. and Weber, F. (1980) Geology and Genesis of the Moanda Manganese Deposits, Republic of Gabon. *The International Geological Congress*, p. 782.

[21] Weber, F. (1993) Les gisements latéritiques de manganèse. In: Paquet, H., Ed., *Sédimentologie et géochimie de la surface*: *Colloque à la mémoire de Georges Millot*, Académie des Sciences, Paris, 77-99.

[22] Gauthier-Lafaye, F. and Weber, F. (2003) Natural Nuclear Fission Reactors: Time Constraints for Occurrence, and Their Relation to Uranium and Manganese Deposits and to the Evolution of the Atmosphere. *Precambrian Research*, **120**, 81-100. https://doi.org/10.1016/S0301-9268(02)00163-8

[23] Maurin, J.C., *et al.* (1991) La chaîne protérozoïque ouest-congolienne et son avant-pays au Congo: Nouvelles données géochronologiques et structurales, implications en Afrique centrale. *Comptes Rendus de l'Académie des Sciences. Série 2*, *Mécanique*, *Physique*, *Chimie*, *Sciences de l'Univers*, *Sciences de la Terre*, **312**, 1327-1334.

[24] Mbina Mounguengui, M. and Guiraud, M. (2009) Neocomian to Early Aptian Syn-Rift Evolution of the Normal to Oblique-Rifted North Gabon Margin (Interior and N'Komi Basins). *Marine and Petroleum Geology*, **26**, 1000-1017. https://doi.org/10.1016/j.marpetgeo.2008.11.001

[25] Seranne, M., Bruguier, O. and Moussavou, M. (2008) U-Pb Single Zircon Grain Dating of Present Fluvial and Cenozoic Aeolian Sediments from Gabon: Consequences on Sediment Provenance, Reworking, and Erosion Processes on the Equatorial West African Margin. *Bulletin de la Société Géologique de France*, **179**, 29-40. https://doi.org/10.2113/gssgfbull.179.1.29

[26] Ledru, P., Eko N'Dong, J., Johan, V., Prian, J.P., Coste, B. and Haccard, D. (1989) Structural and Metamorphic Evolution of the Gabon Orogenic Belt: Collision Tectonics in the Lower Proterozoic? *Precambrian Research*, **44**, 227-241. https://doi.org/10.1016/0301-9268(89)90046-6

[27] Guerrot, C., Feybesse, J. and Johan, V. (1994) Le série de Massima (Gabon): Une greenstone belt archéenne engagée dans la tectonique collisionnelle Protérozoïque inférieur? Implications géotectoniques et paléogéographiques. *Comptes Rendus de l'Académie des Sciences. Série 2*, *Sciences de la Terre et des Planètes*, **318**, 367-374.

[28] Prian, J.P., Eko N'Dong, J. and Coste, B. (1991) Synthèse géologique et géochimique, potentialités minières du degré Carré Mouila: (Archéen et protérozoïque du Gabon Central): Avec carte géologiqe à 1,200 000: Synthèse du district autifère d'Etéké. BRGM, Paris, 212 p.

[29] Bas, M.J.L., Maitre, R.W.L., Streckeisen, A. and Zanettin, B. (1986) A Chemical Classification of Volcanic Rocks Based on the Total Alkali-Silica Diagram. *Journal*

of Petrology, **27**, 745-750. https://doi.org/10.1093/petrology/27.3.745

[30] Cabanis, B. and Lecolle, M. (1989) Le diagramme La/10-Y/15-Nb/8: Un outil pour la discrimination des séries volcaniques et la mise en évidence des processus de mélange et/ou de contamination crustale. *Comptes Rendus de l'Académie des Sciences. Série 2*, *Mécanique*, *Physique*, *Chimie*, *Sciences de l'Univers*, *Sciences de la Terre*, **309**, 2023-2029.

[31] Geringer, G.J. (1979) The Origin and Tectonic Setting of Amphibolites in Part of the Namaqua Metamorphic Belt, South Africa. *South African Journal of Geology*, **82**, 287-303.

[32] Hastie, A.R., Kerr, A.C., Pearce, J.A. and Mitchell, S.F. (2007) Classification of Altered Volcanic Island Arc Rocks using Immobile Trace Elements: Development of the Th-Co Discrimination Diagram. *Journal of Petrology*, **48**, 2341-2357. https://doi.org/10.1093/petrology/egm062

[33] Wood, D.A. (1980) The Application of a Th-Hf-Ta Diagram to Problems of Tectonomagmatic Classification and to Establishing the Nature of Crustal Contamination of Basaltic Lavas of the British Tertiary Volcanic Province. *Earth and Planetary Science Letters*, **50**, 11-30. https://doi.org/10.1016/0012-821X(80)90116-8

[34] Foley, S., Tiepolo, M. and Vannucci, R. (2002) Growth of Early Continental Crust Controlled by Melting of Amphibolite in Subduction Zones. *Nature*, **417**, 837-840. https://doi.org/10.1038/nature00799

[35] Rapp, R.P., Shimizu, N. and Norman, M.D. (2003) Growth of Early Continental Crust by Partial Melting of Eclogite. *Nature*, **425**, 605-609. https://doi.org/10.1038/nature02031

[36] Martin, H., Smithies, R.H., Rapp, R., Moyen, J.F. and Champion, D. (2005) An Overview of Adakite, Tonalite-Trondhjemite-Granodiorite (TTG), and Sanukitoid: Relationships and Some Implications for Crustal Evolution. *Lithos*, **79**, 1-24. https://doi.org/10.1016/j.lithos.2004.04.048

[37] Wang, G.D., Wang, H.Y.C., Chen, H.X., Zhang, B., Zhang, Q. and Wu, C.M. (2017) Geochronology and Geochemistry of the TTG and Potassic Granite of the Taihua Complex, Mts. Huashan: Implications for Crustal Evolution of the Southern North China Craton. *Precambrian Research*, **288**, 72-90. https://doi.org/10.1016/j.precamres.2016.11.006

[38] Middlemost, E.A.K. (1994) Naming Materials in the Magma/Igneous Rock System. *Earth-Science Reviews*, **37**, 215-224. https://doi.org/10.1016/0012-8252(94)90029-9

[39] Peccerillo, A. and Taylor, S.R. (1976) Geochemistry of Eocene Calc-Alkaline Volcanic Rocks from the Kastamonu Area, Northern Turkey. *Contributions to Mineralogy and Petrology*, **58**, 63-81. https://doi.org/10.1007/BF00384745

[40] Maniar, P. and Piccoli, P. (1989) Tectonic Discrimination of Granitoids. *GSA Bulletin*, **5**, 635-643. https://doi.org/10.1130/0016-7606(1989)101%3C0635:TDOG%3E2.3.CO;2 https://pubs.geoscienceworld.org/gsa/gsabulletin/article-abstract/101/5/635/182281/Tectonic-discrimination-of-granitoids

[41] Pearce, J.A., Harris, N.B.W. and Tindle, A.G. (1984) Trace Element Discrimination Diagrams for the Tectonic Interpretation of Granitic Rocks. *Journal of Petrology*, **25**, 956-983. https://doi.org/10.1093/petrology/25.4.956